 doi:10.20944/preprints202211.0010.v1

Article

Radio Emission from Supernova Remnants: Model vs. Observations

Denis Leahy [1], Felicity Merrick [1] and Miroslav Filipović [2,*]

[1] Department of Physics & Astronomy, University of Calgary, Calgary, Alberta T2N 1N4, Canada
[2] Western Sydney University, Locked Bag 1797, Penrith South DC, NSW 1797, Australia
* Correspondence: leahy@ucalgary.ca

Abstract: Supernova remnants (SNRs) are an integral part in studying the properties of the Galaxy and its interstellar medium. For the current work, we explore the relation between the observed radio luminosities of SNRs and the physical properties of those SNRs. The physical properties of 54 SNRs are derived from their observed X-ray spectra. Then the observed radio emission is compared to predicted radio emission using the analytic model of [1]. We find the model can be improved significantly by including an interstellar medium density dependence in the efficiency of particle acceleration and magnetic field amplification.

Keywords: supernova remnants; radio emission

1. Introduction

Supernova remnants (SNRs) are the outcomes of supernova (SN) explosions and provide key insights regarding final stage of stellar evolution, the nature of the interstellar medium (ISM) and energy injection into the Galaxy. The basic classifications of SN are Type Ia and Type II, also referred to as core collapse (CC). Type Ia explosions are produced by the thermonuclear explosion of white dwarfs whereas CC explosions are produced by the collapse of the cores of massive stars at the ends of their lives. Both types are highly energetic and release of order 10^{51} ergs into the surrounding ISM in the form of kinetic energy of one to several solar masses of matter travelling at thousands of km/s. This sudden injection of energy has a significant effect on the ISM, and understanding how this interaction (the SNR) unfolds can provide insight into the evolution of the ISM and the Galaxy as a whole.

SNRs emit over a wide range of wavelengths, radio through gamma-ray (e.g. [2]). Here the topic of study is comparison with data of basic analytic models for the radio emission from SNRs. There are observations of nearly three hundred SNRs in the Galaxy [3]. Understanding of their physical conditions requires models to interpret the observations. E.g., the age of the SNR is a basic characteristic, and is directly known only a handful of SNRs which have historical SN records but is derived for other SNRs using models.

There have been many previous evolutionary models produced for SNRs. They include a simple point explosion in a uniform medium [4], models incorporating radiative energy losses (e.g. [5]), models including effects of the reverse shock in the ejecta at early times [6] and models for the full adiabatic evolution [7]. [7] incorporates results of hydrodynamic simulations. A number of studies (e.g. [8] for Tycho's SNR) use hydrodynamic simulations customized for a specific SNR. A spherically symmetric model developed by [9] and [10] incorporates a number of the above models to calculate SNR evolution from the early ejecta-dominated phase through transition to ISM-dominated phase then to radiative phases. For the non-radiative phases that model uses hydrodynamic simulations to calculate model radii, and temperatures and emission measures for the shocked gas of an SNR. These can be compared to the observed radius and temperature and emission

 doi:10.20944/preprints202211.0010.v1

measure from X-ray observations to deduce explosion energy, age and interstellar medium density of a given SNR.

The radio emission from SNRs is synchrotron emission from electrons accelerated by the SNR shock. An analytic model for radio emission is given by [1], hereafter referred to as the S2017 model. This model uses characteristics such as the shock radius, shock velocity, electron acceleration efficiency, and the magnetic field amplification efficiency to generate a model of the radio luminosity at 1.4 GHz. More complete models have been based on hydrodynamic simulations, such as presented by [14]. The hydrodynamic models are more complex and because of their complexity are difficult to compare to observed radio emission: that comparison of hydrodynamic simulations with observations is an area for future study.

Here we compare the predictions of the S2017 radio emission model with observed SNR radio emission. The SNR variables needed as inputs for the S2017 model are determined using the SNR evolution model of [9]. This paper is organized as follows. We present an updated Table of SNR properties in Section 2, and present the S2017 model in a form suitable for comparison with observed radio emission in Section 3.1. Section 3.2 compares the combined electron acceleration and magnetic field amplication efficiency with values required to match the observed radio emission, to determine what modifications are required. The revised efficiency is presented in Section 3.3, and the results are discussed in Section 4.

2. Physical properties of SNRs

There are 58 Galactic SNRs which have observed X-ray spectra and, from those, forward shock emission measures and shock temperatures. These SNRs were analyzed in two groups to obtain ages, explosion energies and ISM densities: 15 by [11] and 43 by [12]. The results for the 15 SNRs from [11] used an older version of the model [10] so the SNR properties were recalculated using the updated model of [9], which was used by [12]. SNR properties were calculated with the s=0 (uniform ISM density), n=7 (power law index of ejecta density profile) model. For CC, CC? (uncertain CC-type) and "unk." (unknown) type SNRs the ejecta mass was taken as $5M_{\odot}$. For Ia and Ia? (uncertain Ia-type) the ejecta mass was taken as $1.4M_{\odot}$. The errors of the observational inputs were propagated through the model to find the errors of the age, energy, and density. These updated values and errors are given in Table 1 in the Appendix and displayed in Figure 1.

Preprints (www.preprints.org) | NOT PEER-REVIEWED | Posted: 1 November 2022 doi:10.20944/preprints202211.0010.v1

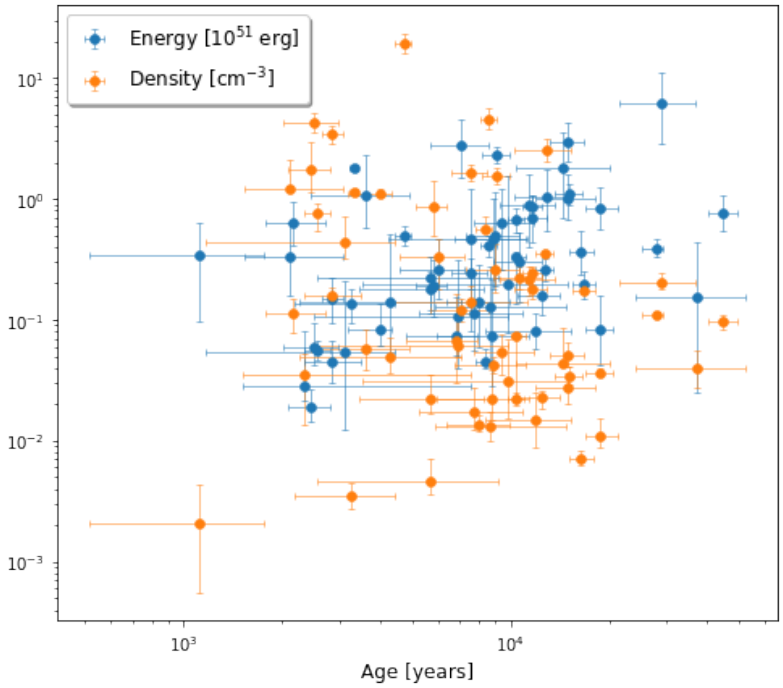

Figure 1. Explosion energy and density of the ISM vs. age for 58 SNRs using models with s = 0, n = 7.

.

The flux densities at 1.4 GHz for the 58 SNRs were gathered from the catalogue of 295 Galactic SNRs by [3]. Those values were given at 1.0 GHz, so the spectral index of each SNRs was used to estimate 1.4 GHz flux densities. If the spectral index of a SNR was unknown, the mean value of all other SNR spectral indices was used. The 1.4 GHz flux densities are included in Table 1. Four of the 58 SNRs had missing values of flux density, so those were excluded from further analysis.

3. Analysis

3.1. Model for Radio Emission at 1.4 GHz

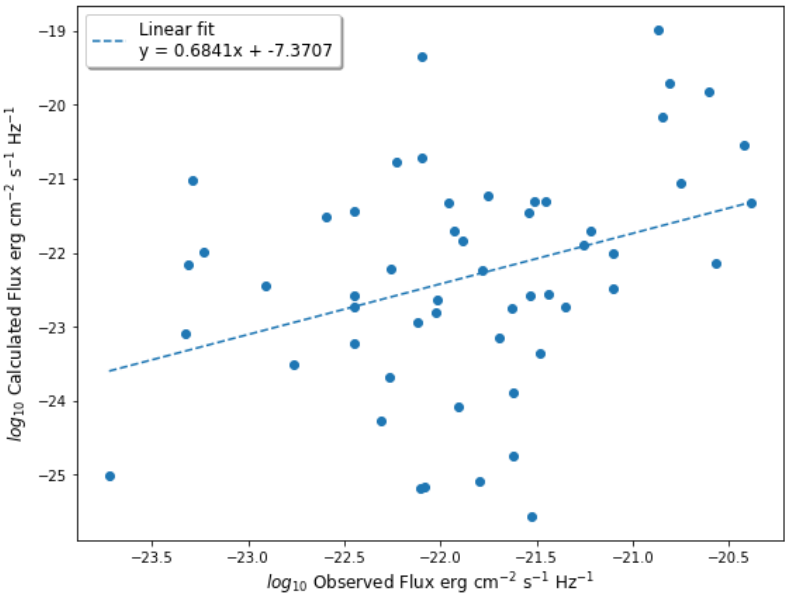

Figure 2. Predicted flux densities of the S2017 model versus observed flux densities for the 58 SNRs..

Preprints (www.preprints.org) | NOT PEER-REVIEWED | Posted: 1 November 2022 doi:10.20944/preprints202211.0010.v1

The radio emission model of [1] (referred to as the S2017 model) is analyzed here. The S2017 model give the radio luminosity density at 1.4 GHz ($L_{1.4}$):

$$L_{1.4} \approx \left(2.2 \times 10^{24} \text{ergs / s / Hz}\right)\left(\frac{R_s}{10 \text{ pc}}\right)^3\left(\frac{\epsilon_e}{10^{-2}}\right)\left(\frac{\epsilon_b^u}{10^{-2}}\right)^{0.8}\left(\frac{v_s}{500 \text{ km/s}}\right)^{3.2} \quad (1)$$

where R_s is the shock radius, ϵ_e is the fraction of shock energy from relativistic electrons, referred to as the electron acceleration efficiency, ϵ_b^u is the fraction of shock energy in an amplified upstream magnetic field, referred to as the magnetic field amplification efficiency, and v_s is the shock velocity. The magnetic field amplification efficiency is calculated [1] using:

$$\epsilon_b^u = \frac{\xi_{cr}}{2}\left(\frac{v_s}{c} + \frac{9\mu G}{v_s\sqrt{4\pi n_0}}\left(\frac{n_0}{1.6E-27 \text{ g cm}^{-3}}\right)^{0.47}\right) \quad (2)$$

where ξ_{cr} is the cosmic ray acceleration efficiency. The value of $\xi_{cr} = 0.1$ was used in S2017. μ is 0.61 m_H, G is the gravitational constant, and n_0 is the density of the local interstellar medium.

We rearrange Equation 1 to yield the radio flux density at 1.4 GHz:

$$F_{1.4} \approx \left(\frac{2.2 \times 10^{24}}{4\pi} \text{ ergs/ s / Hz}\right)\theta^3\left(\frac{d}{(10 \text{ pc})^3}\right)\left(\frac{\epsilon_e}{10^{-2}}\right)\left(\frac{\epsilon_b^u}{10^{-2}}\right)^{0.8}\left(\frac{v_s}{500 \text{ km/s}}\right)^{3.2} \quad (3)$$

where θ is the angular size of the supernova remnant and d is the distance to the supernova remnant. By using angular size, which is well measured, rather than shock radius we reduce the impact of errors of distance.

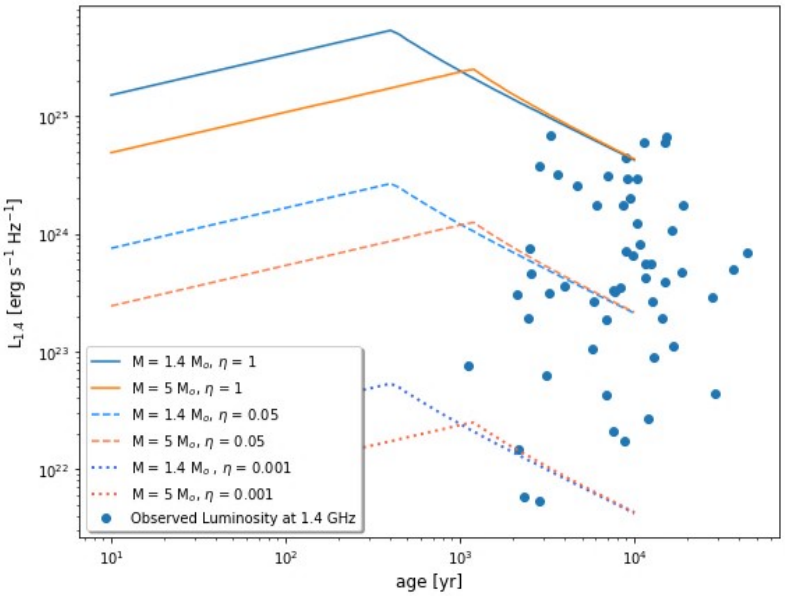

Figure 3. luminosity equation versus observed luminosity with constant eta values. M = 1.4 curves correspond to Ia SNRs. M = 5 curves correspond to CC SNRs. Shock velocity and radius calculated with E of 10^{51} erg and n_0 of 1 cm^{-3}.

The predicted flux densities of the SNRs for $\epsilon_e = 4.2 \times 10^{-3}$ used in the S2017 model, are compared to the observed flux densities in Figure 2. The predicted values are poorly correlated with the observed ones, with predicted flux densities scattered over a factor of 10^6, compared to a $\sim 10^3$ range for the observed values. This implies that the model is missing important factors or that the model can be improved by changing some of the assumptions.

To check that the S2017 model can produce the same range of radio luminosities as the observed one, we calculate the S2017 luminosity vs. age by using the shock velocity and

Preprints (www.preprints.org) | NOT PEER-REVIEWED | Posted: 1 November 2022 doi:10.20944/preprints202211.0010.v1

shock radius vs. age from the SNR model of [9]. The explosion energy was fixed at 10^{51} erg, the local interstellar density was fixed at 1 cm^{-3} and the ejecta mass was 1.4 or 5 $M_{\odot}$. The combined efficiency, η, is defined as:

$$\eta = \left(\frac{\epsilon_e}{10^{-2}}\right)\left(\frac{\epsilon_b^u}{10^{-2}}\right)^{0.8} \quad (4)$$

Three values for η were used to produce the set of radio luminosity evolution curves in Figure 3.

From Figure 3 it is seen that η has a range of approximately three orders of magnitude. If ϵ_e is approximated to be equal to ϵ_b^u this gives us $\epsilon_e \sim 10^{-4}$ to 10^{-2}. This values can be compared to $\epsilon_e = 4.2 \times 10^{-3}$ chosen in the S2017 model.

3.2. Analysis of the Efficiency

To examine how to improve the S2017 model, we start by analysis of the efficiency. We test whether a dependence of the efficiency on SNR properties can improve the agreement between model and observations. The combined efficiency η can be inserted into Equation 3 to yield:

$$F_{1.4} \approx \left(\frac{2.2 \times 10^{24}}{4\pi}\text{ergs / s / Hz}\right)\theta^3\left(\frac{d}{(10\text{ pc})^3}\right)\eta\left(\frac{v_s}{500\text{km/s}}\right)^{3.2} \quad (5)$$

The combined efficiency η required to reproduce the observed radio emission using Equation 5 is compared to SNR properties. The η vs. shock velocity, density, and shock radius revealed the trends shown in Figure 4. The fit lines are a least-squares linear regression (in log-log space), corresponding to the best fit power law relation for the variables. Figure 4 shows that η is approximately proportional to v_s^{-3} , n_0^1 , and R_s^{-2}. This is indicates a dependence on the density of the ISM which is not present in the S2017 model.

The shock radius is global property of each SNR, and should have no effect on the efficiency which should depend on local variables. As a result, the relation between η and the shock radius is likely a consequence of η dependence on the shock velocity and ISM density.

3.3. Efficiency dependence on shock velocity and ISM density

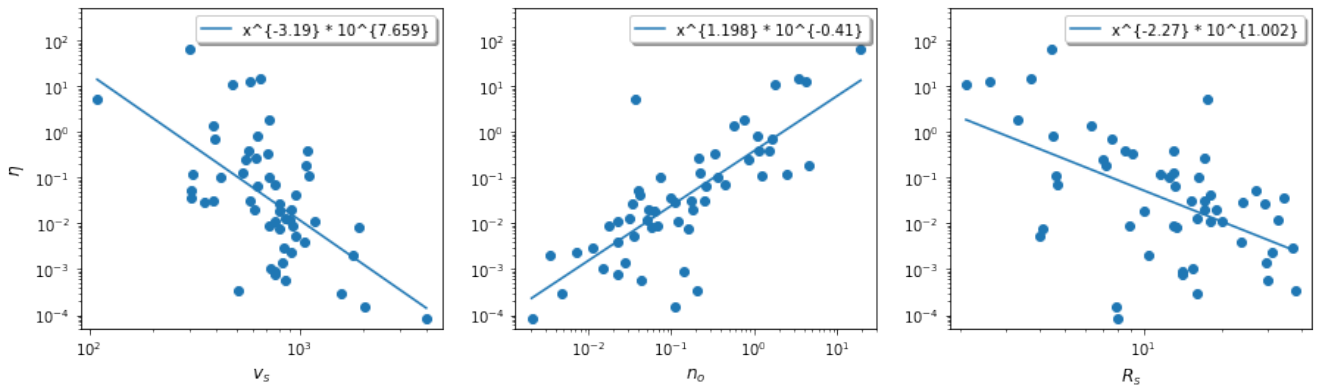

Figure 4. a) η vs shock velocity v_s of each SNR. (**b**) η vs density n_0. (**c**) η vs shock radius R_s .

Preprints (www.preprints.org) | NOT PEER-REVIEWED | Posted: 1 November 2022 doi:10.20944/preprints202211.0010.v1

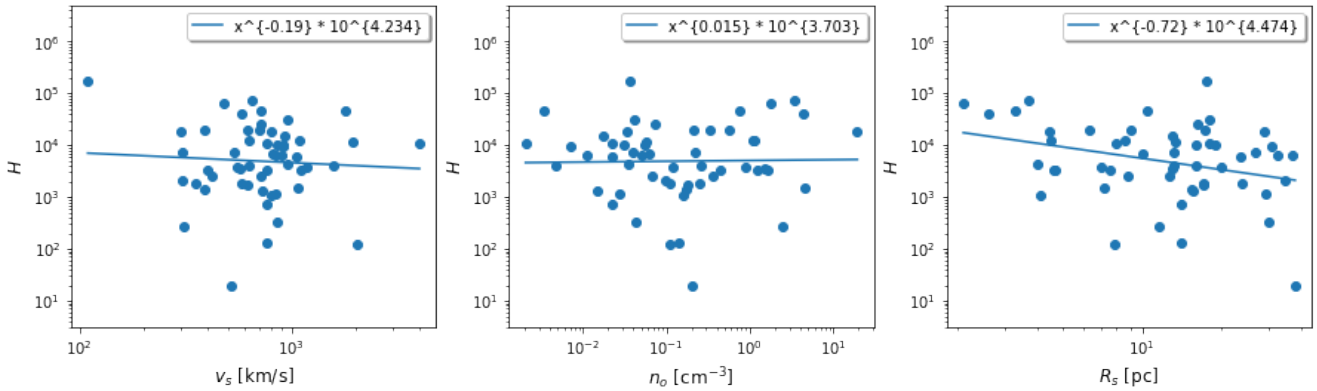

Figure 5. a) H vs shock velocity v_s of each SNR. (**b**) H vs density n_0. (**c**) H vs shock radius R_s.

The correlation between η and shock velocity and density is modelled by introducing an explicit power-law dependence:

$$\eta \quad = H\, n_0^{\alpha}\, v_s^{\beta}$$

where H is new parameter. The values of α and β were varied to achieve no significant correlation between H and shock velocity or density. The best fit values were $\alpha \simeq 1$ and $\beta \simeq -3/2$, which means that η is approximately proportional to n_0 and $v_s^{-3/2}$.

These values result in the correlations between H and shock velocity and density shown in Figure 5. There is no remaining correlation of H with density and velocity, as expected. By introducing the density and velocity dependences, the correlation of H with shock radius is much reduced, compared with the original corrlation of η with radius. The scatter of H vs. n_0, vs. v_s and vs. R_s is much reduced, indicating that most of the efficiency dependence on SNR parameters has been captured. In summary we find that there is an empirical relationship between the efficiency, and thus the 1.4 GHz luminosity of a SNR, and the density of the local ISM, and that the velocity dependence is much weaker than in the S2017 model.

4. Discussion

This investigation revealed that the model proposed by [1], which is described in equation 1, cannot be verified. Although the existence of many parameters enabled the data to be fit to observations, this fit required a large range of variance in the efficiency parameters.

The statistical study of radio emission from SNRs by [13] found that the models of constant efficiencies of particle acceleration and magnetic field amplification do not fit the data well. In addition, they showed that the cumulative size distribution of SNRs is related to the ambient density distribution.

More significantly, this investigation revealed a dependence on the density of the local interstellar medium which was not present in this model originally. This dependence on density has been confirmed in other models. Specifically, it is explored in hydrodynamic simulations investigated by [14]. These results show that the proposed model might be too simplified to model the SNRs in the Galaxy.

SNRs reveal valuable insight into the Galaxy and the interstellar medium. Due to limitations in observations, models are used to obtain data on many of the characteristics of these remnants.

This investigation examined the model of SNRs proposed by [1], which relates the radio luminosity at 1.4 GHz to the shock radius, electron acceleration efficiency, magnetic field amplification efficiency, and the shock velocity. It found that when the model is compared against observations of 54 SNRs in the Galaxy, the results are inconsistent. A further investigation into the results revealed a dependence on density which is not present

 doi:10.20944/preprints202211.0010.v1

in the original model, suggesting the model may be too simplified. Additional exploration into hydrodynamic simulations would be beneficial to obtain a greater understanding in regard to the extent by which complex models of SNRs can be simplified to reveal otherwise unobtainable characteristics of the remnants and their surrounding environments.

Preprints (www.preprints.org) | NOT PEER-REVIEWED | Posted: 1 November 2022 doi:10.20944/preprints202211.0010.v1

Table 1. Observed and Calculated Quantities of 58 SNRs.

Name	Type[1]	Age [10^2 yrs]	Energy [10^{50} erg]	Density [10^{-2}cm^{-3}]	Shock Radius [pc]	Shock Velocity [km/s]	Distance [kpc]	1.4GHz flux density [Jy][2]
G 38.7-1.3	CC?	86^{+60}_{-27}	$1.27^{+1.45}_{-0.84}$	$1.32^{+0.43}_{-0.31}$	14.9^{+3}_{-3}	960^{+610}_{-290}	$4^{+4.8}_{-3.2}$	? [3]
G 53.6-2.2	Ia	446^{+46}_{-45}	$7.65^{+2.93}_{-2.24}$	$9.62^{+1.46}_{-1.19}$	$34.6^{+3.6}_{-3.6}$	310^{+750}_{-20}	$7.8^{+8.6}_{-7}$	9.47
G 67.7+1.8	CC?	23^{+53}_{-8}	$0.28^{+0.54}_{-0.07}$	$3.53^{+1.73}_{-2.16}$	4^{+7}_{-1}	950^{+340}_{-380}	$2^{+5.7}_{-1.2}$	1.23
G 78.2+2.1	CC?	94^{+23}_{-16}	$6.29^{+5.81}_{-3.73}$	$5.41^{+2.10}_{-1.94}$	19^{+4}_{-4}	910^{+130}_{-13}	$2.1^{+2.5}_{-1.3}$	380.
G 82.2+5.3	unk. [b]	189^{+25}_{-19}	$8.26^{+4.27}_{-2.67}$	$1.10^{+0.41}_{-0.21}$	37^{+4}_{-4}	850^{+60}_{-70}	$3.2^{+3.6}_{-2.4}$	142.
G 84.2-0.8	unk. [b]	124^{+18}_{-18}	$1.59^{+0.96}_{-0.51}$	$2.26^{+0.34}_{-0.44}$	18^{+3}_{-3}	76^{+110}_{-80}	$6^{+6.2}_{-5.2}$	13.0
G 85.4+0.7	CC?	57^{+26}_{-22}	$1.79^{+0.73}_{-0.59}$	$2.20^{+1.36}_{-0.51}$	12^{+4}_{-4}	1180^{+280}_{-180}	$3.5^{+4.5}_{-2.7}$	? [3]
G 85.9-0.6	Ia?	80^{+19}_{-15}	$1.4^{+1.42}_{-0.81}$	$1.36^{+0.29}_{-0.17}$	17^{+5}_{-5}	1010^{+180}_{-140}	$4.8^{+6.4}_{-4}$	? [3]
G 89.0+4.7	CC	164^{+16}_{-12}	$3.64^{+1.75}_{-1.27}$	$0.71^{+0.12}_{-0.09}$	31^{+4}_{-4}	910^{+60}_{-60}	$1.9^{+2.2}_{-1.1}$	250.
G 109.1-1.0	CC	127^{+80}_{-80}	$2.6^{+0.60}_{-0.51}$	$35.59^{+2.45}_{-2.05}$	$12.6^{+0.9}_{-0.9}$	420^{+20}_{-10}	$3.1^{+3.3}_{-2.3}$	23.3
G 116.9+0.2	CC	167^{+14}_{-13}	$1.98^{+0.55}_{-0.47}$	$17.50^{+0.99}_{-0.86}$	$15.3^{+1.5}_{-1.5}$	390^{+20}_{-20}	$3.1^{+3.4}_{-2.3}$	9.69
G 132.7+1.3	unk. [b]	279^{+13}_{-27}	$3.83^{+0.85}_{-0.48}$	$10.89^{+0.32}_{-0.30}$	$24^{+1.2}_{-1.2}$	350^{+20}_{-10}	$2.1^{+2.2}_{-1.3}$	55.1
G 156.2+5.7	CC	291^{+75}_{-76}	$61.2^{+48.3}_{-32.2}$	$20.38^{+3.91}_{-2.63}$	38^{+10}_{-10}	510^{+100}_{-70}	$2.5^{+3.3}_{-1.7}$	5.92
G 160.9+2.6	CC?	57^{+35}_{-31}	$2.23^{+1.1}_{-1.11}$	$0.47^{+0.23}_{-0.10}$	16^{+8}_{-8}	1570^{+640}_{-290}	$0.8^{+1.2}_{-0}$	136.
G 166.0+4.3	unk.	145^{+56}_{-41}	$17.8^{+17.4}_{-10.8}$	$4.37^{+4.25}_{-0.11}$	30^{+9}_{-9}	850^{+200}_{-160}	$4.5^{+6}_{-3.7}$	7.93
G 260.4-3.4	CC	33^{+11}_{-11}	$1.34^{+0.45}_{-0.41}$	$0.35^{+0.10}_{-0.07}$	10.5^{+3}_{-3}	1800^{+330}_{-690}	$1.3^{+1.6}_{-0.5}$	154.
G 272.2-3.2	Ia	75^{+38}_{-33}	$4.64^{+7.56}_{-3.84}$	$14.1^{+4.94}_{-2.71}$	14^{+7}_{-7}	760^{+340}_{-200}	$6^{+10}_{-5.2}$	0.49
G 296.7-0.9	unk.	116^{+13}_{-13}	$6.9^{+3.85}_{-2.52}$	$18.0^{+4.83}_{-3.28}$	17^{+2}_{-2}	610^{+50}_{-50}	$10^{+10.9}_{-9.2}$	3.55
G 296.8-0.3	CC?	104^{+6}_{-5}	$6.76^{+1.65}_{-1.46}$	$2.23^{+0.26}_{-0.27}$	$23.7^{+1.5}_{-1.5}$	1050^{+40}_{-40}	$9.6^{+10.2}_{-8.8}$	11.0
G 299.2-2.9	Ia	88^{+26}_{-28}	$0.74^{+1.4}_{-0.45}$	$2.23^{+1.60}_{-0.75}$	14^{+5}_{-5}	770^{+280}_{-130}	$5^{+6}_{-4.2}$	0.59
G 304.6+0.1	unk.	89^{+23}_{-21}	$4.62^{+5.34}_{-2.84}$	$4.21^{+0.77}_{-0.62}$	18^{+6}_{-6}	960^{+220}_{-140}	$15^{+20}_{-14.2}$	16.6
G 306.3-0.9	Ia	128^{+25}_{-25}	$10.2^{+7.25}_{-4.79}$	$250.16^{+59.75}_{-43.83}$	$11.6^{+2.3}_{-2.3}$	310^{+60}_{-40}	$20^{+24}_{-19.2}$	0.19
G 308.4-1.4	CC?	29^{+60}_{-5}	$0.44^{+0.22}_{-0.15}$	$16.03^{+2.30}_{-2.18}$	$4.1^{+0.5}_{-0.5}$	800^{+100}_{-90}	$3.1^{+3.4}_{-2.3}$	0.47
G 309.2-0.6	CC?	11^{+60}_{-6}	$3.43^{+2.85}_{-2.46}$	$0.21^{+0.23}_{-0.15}$	8^{+4}_{-4}	4010^{+1570}_{-1220}	$2.8^{+3.6}_{-2}$	8.01
G 311.5-0.3	unk.	69^{+29}_{-44}	$1.07^{+2.01}_{-0.68}$	$6.21^{+4.45}_{-1.33}$	10^{+6}_{-6}	810^{+440}_{-200}	$6.6^{+13.6}_{-5.8}$	3.55
G 315.4-2.3	Ia	116^{+8}_{-8}	$8.49^{+2.05}_{-1.79}$	$24.75^{+2.79}_{-2.71}$	$17^{+1.1}_{-1.1}$	580^{+30}_{-30}	2.8^{+3}_{-2}	60.0
G 322.1+0.0	CC	43^{+28}_{-20}	$1.4^{+3.65}_{-0.89}$	$4.99^{+2.19}_{-1.41}$	$8.5^{+0.8}_{-0.8}$	1110^{+490}_{-270}	$9.3^{+10.2}_{-8.5}$	? [3]
G 327.4+0.4	unk.	106^{+19}_{-17}	$2.99^{+2.34}_{-1.59}$	$22.47^{+4.83}_{-4.47}$	$13.1^{+2.7}_{-2.7}$	540^{+70}_{-60}	$4.3^{+5.1}_{-3.5}$	36.7
G 330.0+15	unk.	371^{+151}_{-131}	$1.52^{+2.82}_{-1.27}$	$3.98^{+1.66}_{-1.27}$	27^{+12}_{-12}	310^{+100}_{-80}	$1^{+1.5}_{-0.5}$	414.
G 330.2+1.0	CC	98^{+52}_{-63}	$1.97^{+13.3}_{-1.18}$	$3.15^{+3.69}_{-1.60}$	16^{+8}_{-8}	860^{+550}_{-240}	10^{+15}_{-5}	5.53
G 332.4-0.4	CC?	40^{+3}_{-8}	$0.83^{+0.55}_{-0.22}$	$110.05^{+10.10}_{-7.06}$	$4.5^{+0.9}_{-0.9}$	630^{+60}_{-50}	$3^{+3.3}_{-2.7}$	33.1
G 332.4+0.1	unk.	70^{+16}_{-14}	$27.4^{+17.9}_{-12.5}$	$11.87^{+02.98}_{-2.19}$	20^{+4}_{-4}	1180^{+180}_{-140}	$9.2^{+10.9}_{-7.5}$	30.8
G 332.5-5.6	unk.	120^{+33}_{-35}	$0.81^{+0.33}_{-0.23}$	$1.48^{+1.07}_{-0.61}$	15.5^{+4}_{-4}	720^{+120}_{-70}	$3^{+3.8}_{-2.2}$	2.53
G 337.2-0.7	Ia?	31^{+13}_{-19}	$0.55^{+1.55}_{-0.43}$	$44.23^{+27.15}_{-11.65}$	4.7^{+3}_{-3}	760^{+540}_{-210}	5.5^{+9}_{-2}	1.72
G 337.8-0.1	CC?	36^{+13}_{-12}	$10.6^{+12.4}_{-4.85}$	$5.75^{+2.55}_{-1.84}$	$13.4^{+1.3}_{-1.3}$	1930^{+520}_{-400}	$12.3^{+13.5}_{-11.1}$	17.7
G 347.3-0.5	CC	68^{+11}_{-20}	$0.73^{+0.80}_{-0.22}$	$6.75^{+9.40}_{-3.78}$	$8.8^{+1.7}_{-1.7}$	720^{+17}_{-80}	$1^{+1.2}_{-0.8}$	35.3
G 348.5+0.1	CC	114^{+22}_{-21}	$8.77^{+6.96}_{-4.72}$	$21.57^{+5.81}_{-5.61}$	$17.2^{+3.5}_{-3.5}$	620^{+90}_{-100}	$7.9^{+9.5}_{-6.3}$	79.6
G 348.7+0.3	CC	149^{+19}_{-18}	$29.5^{+13.}_{-8.87}$	$5.07^{+1.38}_{-0.93}$	$32.8^{+3.3}_{-3.3}$	890^{+70}_{-60}	$13.2^{+14.5}_{-11.9}$	28.8
G 349.7+0.2	CC	29^{+2}_{-2}	$1.5^{+0.74}_{-0.56}$	$343.79^{+54.59}_{-55.68}$	$3.7^{+0.4}_{-0.4}$	650^{+40}_{-40}	$11.5^{+12.7}_{-10.3}$	23.7
G 350.1-0.3	CC	25^{+5}_{-5}	$0.60^{+0.34}_{-0.17}$	$428.43^{+90.78}_{-74.91}$	$2.6^{+0.5}_{-0.5}$	580^{+70}_{-50}	$9^{+10.8}_{-7.2}$	7.85
G 352.7-0.1	Ia?	76^{+9}_{-10}	$2.44^{+0.81}_{-0.64}$	$165.61^{+24.59}_{-25.27}$	$7.6^{+0.5}_{-0.5}$	400^{+40}_{-50}	7.5^{+8}_{-7}	4.89
G 355.6-0.0	unk.	90^{+17}_{-17}	$4.91^{+6.45}_{-3}$	$25.91^{+16.79}_{-9.18}$	$13.2^{+2.7}_{-2.7}$	630^{+100}_{-90}	$13^{+15.6}_{-10.4}$	3.53
G 359.1-0.5	unk.	187^{+20}_{-17}	$0.84^{+0.73}_{-0.41}$	$3.61^{+0.34}_{-0.17}$	$17.5^{+3.5}_{-3.5}$	110^{+120}_{-30}	5^{+6}_{-4}	16.0
G 18.1-0.1	unk.	58^{+5}_{-7}	$1.89^{+1.2}_{-0.83}$	$87.3^{+55.7}_{-38.4}$	$7^{+0.2}_{-0.2}$	550^{+80}_{-60}	$6.4^{+6.6}_{-6.2}$	5.44

[1] CC, CC? and "unk." (unknown type) SNRs are taken to have $5M_\odot$ ejecta mass; Ia and Ia? are taken to have $1.4M_\odot$ ejecta mass. [2] 1 Jy is 10^{-23}erg cm^{-2} s^{-1} Hz^{-1}. [3] 1.4 GHz flux density;"?" denotes SNRs without known 1.4 GHz flux density: these are omitted for this analysis.

Preprints (www.preprints.org) | NOT PEER-REVIEWED | Posted: 1 November 2022 doi:10.20944/preprints202211.0010.v1

Table 2. Observed and Calculated Quantities of 58 SNRs (Table 1 continued).

Name	Type[1]	Age [10^2 yrs]	Energy [10^{50} erg]	Density [10^{-2}cm^{-3}]	Shock Radius [pc]	Shock Velocity [km/s]	Distance [kpc]	1.4GHz flux density [Jy][2]
G 21.5-0.9	CC	25^{+4}_{-4}	$0.19^{+0.07}_{-0.05}$	176^{+120}_{-61}	$2.1^{+0.1}_{-0.1}$	480^{+40}_{-40}	$4.4^{+4.6}_{-4.2}$	8.23
G 21.8-0.6	unk.	104^{+7}_{-3}	$3.37^{+0.23}_{-2.02}$	$7.44^{+0.43}_{-5.3}$	$16.3^{+0.6}_{-0.6}$	710^{+250}_{-80}	$5.6^{+5.8}_{-5.4}$	78.5
G 27.4+0.0	CC	21^{+10}_{-6}	$3.34^{+2.96}_{-1.75}$	$122^{+85}_{-1.25}$	$4.6^{+0.25}_{-0.25}$	1110^{+220}_{-290}	$5.8^{+6.1}_{-5.5}$	7.54
G 28.6-0.1	unk.	149^{+32}_{-30}	$10.1^{+5.8}_{-3.28}$	$2.79^{+0.79}_{-0.79}$	$29.3^{+0.9}_{-0.9}$	840^{+110}_{-100}	$9.6^{+9.9}_{-9.3}$	3.53
G 29.7-0.3	CC	26^{+2}_{-2}	$0.56^{+0.10}_{-0.09}$	$75.7^{+17}_{-22.2}$	$3.3^{+0.15}_{-0.15}$	720^{+40}_{-40}	$5.6^{+5.9}_{-5.3}$	12.4
G 31.9+0.0	CC	86^{+5}_{-5}	$4.06^{+0.91}_{-0.7}$	453^{+104}_{-80}	$7.2^{+0.4}_{-0.4}$	1070^{+20}_{-20}	$7.1^{+7.5}_{-6.7}$	29.4
G 32.8-0.1	unk.	78^{+31}_{-25}	$1.12^{+1.35}_{-0.55}$	$1.75^{+0.99}_{-0.52}$	$13^{+0.8}_{-0.8}$	930^{+240}_{-170}	$4.8^{+5.1}_{-4.5}$	11.8
G 33.6+0.1	CC	84^{+4}_{-5}	$0.45^{+0.12}_{-0.05}$	$56.5^{+15.3}_{-4.6}$	$6.3^{+0.4}_{-0.4}$	390^{+20}_{-30}	$3.5^{+3.8}_{-3.2}$	23.7
G 34.7-0.4	unk.	90^{+9}_{-9}	$23.1^{+3.4}_{-3.4}$	154^{+26}_{-21}	$13^{+1.3}_{-1.3}$	580^{+40}_{-30}	$3^{+3.3}_{-2.7}$	272.
G 39.2-0.3	CC	60^{+12}_{-15}	$2.62^{+1.97}_{-1.12}$	$33.7^{+12.7}_{-15.5}$	$9.1^{+0.5}_{-0.5}$	710^{+160}_{-90}	8.5^{+9}_{-8}	20.2
G 41.1-0.3	Ia	47^{+3}_{-3}	$4.93^{+0.97}_{-0.82}$	1940^{+390}_{-330}	$4.45^{+0.25}_{-0.25}$	300^{+20}_{-20}	8.5^{+9}_{-8}	29.6
G 43.3-0.2	unk.	33^{+1}_{-1}	17.8^{+1}_{-1}	115^{+7}_{-5}	$8.55^{+0.3}_{-0.3}$	1090^{+20}_{-20}	$11.3^{+11.7}_{-10.9}$	44.4
G 49.2-0.7	CC	152^{+14}_{-15}	$11.^{+2.1}_{-2.01}$	$3.38^{+0.66}_{-0.5}$	$29^{+3.3}_{-3.3}$	800^{+60}_{-40}	$5.6^{+6.2}_{-5}$	177.
G 54.1+0.3	CC	22^{+6}_{-4}	$6.4^{+2.93}_{-2.33}$	$11.2^{+3.5}_{-3.41}$	$7.9^{+1.3}_{-1.3}$	2040^{+230}_{-250}	$4.9^{+5.7}_{-4.1}$	0.52

[1] CC, CC? and "unk." (unknown type) SNRs are taken to have $5M_\odot$ ejecta mass; Ia and Ia? are taken to have $1.4M_\odot$ ejecta mass. [2] 1 Jy is 10^{-23}erg cm^{-2} s^{-1} Hz^{-1}. [3] 1.4 GHz flux density;"?" denotes SNRs without known 1.4 GHz flux density: these are omitted for this analysis.

Author Contributions: Conceptualization, D.L. and M.F.; methodology, D.L.; software, D.L. and F.M.; analysis, D.L. and F.M.; writing—original draft preparation, F.M. and D.L.; writing—review and editing, D.L. and M.F.; funding acquisition, D.L. All authors have read and agreed to the published version of the manuscript.

Funding: This research was funded by the Natural Sciences and Engineering Research Council of Canada.

Conflicts of Interest: The authors declare no conflict of interest. The funders had no role in the design of the study; in the collection, analyses, or interpretation of data; in the writing of the manuscript; or in the decision to publish the results.

Abbreviations

The following abbreviations are used in this manuscript:

SNR	supernova remnant
ISM	interstellar medium
CC	core collapse

References

1. Sarbadhicary, S., Badenes, C., Chomiuk, L., Caprioli, D., Huizenga, D. Supernova remnants in the Local Group - I. A model for the radio luminosity function and visibility times of supernova remnants. *Monthly Notices of the R.A.S.* **2018**, *464*, 2326–2340.
2. Dubner, G., Giacani, E. Radio emission from supernova remnants. *Astron. Astrophys. Review* **2015**, *23*, 3.
3. Green, D. A. A revised catalogue of 294 Galactic supernova remnants. *J. Astrophys. Astron.* **2019**, *40*, 36.
4. Sedov, L. I. *Similarity and Dimensional Methods in Mechanics*; Editor 1, F., Editor 2, A., Eds.; Academic Press: New York, U.S.A, 1959.
5. Cioffi, D.,McKee, C.,Bertschinger, E. Dynamics of Radiative Supernova Remnants. *Astrophys. J.* **1988**, *334*, 252.
6. Chevalier, R. A. Self-similar solutions for the interaction of stellar ejecta with an external medium. *Astrophys. J.* **1982**, *258*, 790–797.
7. Truelove, J., McKee, C. Evolution of Nonradiative Supernova Remnants. *Astrophys. J. Supp.* **1999**, *120*, 299–326.
8. Badenes, C., Borkowski, K., Hughes, J., Hwang, U., Bravo, E. Constraints on the Physics of Type Ia Supernovae from the X-Ray Spectrum of the Tycho Supernova Remnant. *Astrophys. J.* **2006**, *645*, 1373–1391.
9. Leahy, D., Wang, Y., Lawton, B., Ranasinghe, S., Filipović, M. Emission Measures and Emission-measure-weighted Temperatures of Shocked Interstellar Medium and Ejecta in Supernova Remnants. *Astron. J.* **2019**, *158*, 149.
10. Leahy, D., Williams, J. A Python Calculator for Supernova Remnant Evolution. *Astron. J.* **2017**, *153*, 239.

 doi:10.20944/preprints202211.0010.v1

11. Leahy, D., Ranasinghe, S. Evolutionary Models for 15 Galactic Supernova Remnants with New Distances. *Astrophys. J.* **2018**, *866*, 9.
12. Leahy, D., Ranasinghe, S., Gelowitz, M. Evolutionary Models for 43 Galactic Supernova Remnants with Distances and X-Ray Spectra. *Astrophys. J. Supp.* **2020**, *248*, 16.
13. Bandiera, R., Petruk, O. A statistical approach to radio emission from shell-type SNRs. I. Basic ideas, techniques, and first results. *Astron. Astrophys.* **2010**, *509*, A34.
14. Pavlović, M., Urošević, D., Arbutina, B., Orlando, S., Maxted, N., Filipović, M. Radio Evolution of Supernova Remnants Including Nonlinear Particle Acceleration: Insights from Hydrodynamic Simulations. *Astrophys. J.* **2018**, *852*, 84.